Cell Biol Toxicol (2024) 40:108
https://doi.org/10.1007/s10565-024-09941-x

RESEARCH

The mechanism of sevoflurane affecting ovarian cancer cell proliferation and migration by regulating RNA methylase TRDMT1 to activate the β-catenin pathway

Xiaochen Huang · Xuewei Lao · Chengyan He · Jia Wang · Ying Pan

Received: 6 June 2024 / Accepted: 28 October 2024

Abstract

Objective Sevoflurane (Sevo), a commonly used inhalant anesthetic clinically, is associated with a worsened cancer prognosis, and we investigated its effect on RNA methylase tRNA aspartic acid methyltransferase 1 (TRDMT1) expression and ovarian cancer (OC) cell malignant phenotypes.

Methods Human OC cells (OVCAR3/SKOV3) were pretreated with 3.6% Sevo and cultured under normal conditions for 48 h, with their viability assessed. After 2-h Sevo treatment or interference plasmid transfections to down-regulate TRDMT1/adenomatous polyposis coli (APC), changes in TRDMT1, APC and β-catenin expression, cell proliferative activity, cycle, apoptosis, migration, invasion, and 5-methylcytosine (m5C) methylation potential modification sites were evaluated. Additionally, APC mRNA m5C methylation level and stability, the binding of APC mRNA with TRDMT1, the binding intensity of APC and β-catenin, and β-catenin nuclear translocation were detected Lastly, Cyclin D1, cellular-myelocytomatosis viral oncogene (C-myc) and β-catenin protein levels, and ki67-positive rate were assessed.

Results Sevo treatment boosted cell cycle, proliferation, migration and invasion, suppressed apoptosis and APC expression, and up-regulated C-myc, β-catenin, TRDMT1 and Cyclin D1 levels. Silencing TRDMT1 or β-catenin partially averted Sevo-mediated promotion effects on cell malignant biological behaviors. Lowly-expressed APC annulled the effect of silencing TRDMT1 and promoted cell malignant behaviors. Sevo enhanced APC mRNA m5C modification and degradation and activated the APC/β-catenin pathway by increasing TRDMT1, thus encouraging OC growth in vivo.

Conclusions Sevo stimulated APC m5C modification and curbed its expression by up-regulating TRDMT1, which in turn activated the β-catenin pathway to stimulate OC cell cycle, invasion, proliferation, and migration and to suppress apoptosis.

Keywords Sevoflurane · Ovarian cancer · TRNA aspartic acid methyltransferase 1 · 5-methylcytosine · Adenomatous polyposis coli · β-catenin · Cellular-myelocytomatosis viral oncogene · Cyclin D1

Xiaochen Huang and Xuewei Lao contributed equally to this work.

Supplementary information The online version contains supplementary material available at https://doi.org/10.1007/s10565-024-09941-x.

X. Huang · C. He
Clinical Laboratory, The Third Bethune Hospital of Jilin University, Changchun, China

X. Lao · J. Wang · Y. Pan (✉)
Department of Gynecology, The Third Bethune Hospital of Jilin University, No.126, Xiantai Avenue, Changchun 130033, China
e-mail: panying@jlu.edu.cn

Published online: 04 December 2024

Introduction

Ovarian cancer (OC) is the eighth most commonly diagnosed carcinoma and the eighth primary reason for cancer-associated mortality among women on a global scale (Atallah et al. 2021). The primary therapeutic approach for OC involves the surgical removal of solid tumors, but postoperative recurrence remains the main reason for mortality (Angeles et al. 2022). Existing research has shown that the administration of perioperative anesthetics may be a risk factor for cancer recurrence, particularly for inhaled anesthetics, which negatively impact cancer prognosis (Enlund et al. 2014; Heaney and Buggy 2012; Horowitz et al. 2015). Sevoflurane (Sevo) is the most widely employed inhalant anesthetic, yet it has been linked to a worsened cancer prognosis and recurrence (Enlund et al. 2014; Takeyama et al. 2021). There is previous evidence implying that Sevo can inhibit the proliferation and metastasis of OC (Zhang et al. 2019; Kang and Wang 2019). Conversely, short-term (such as 2 h) Sevo treatment has been documented to enhance OC cell malignancy, proliferation, and metastasis (Ishikawa et al. 2021; Iwasaki et al. 2016). Additionally, Sevo can strengthen OC cell biological malignant behaviors by modulating cell metabolism and signal transduction mechanisms (Hu et al. 2023). However, the mechanism of Sevo facilitating OC malignant behaviors has not been fully elucidated.

tRNA aspartic acid methyltransferase 1 (TRDMT1), also named DNA methyltransferase-2 (DNMT2), is a regulatory factor engaged in the stress response, cell proliferation and survival, which possesses the ability to regulate cellular stress responses like oxidative stress, salt stress, inflammatory response, and drug-induced cell senescence (Bloniarz et al. 2021; Li et al. 2022; Thiagarajan et al. 2011). In human cervical cancer cells, impaired nucleolar activity mediated by nano-diamond is accompanied by oxidative stress and TRDMT1 upregulation, which may aid in RNA stability and mitigate stress-induced RNA damage by methylating RNA (Mytych et al. 2014). Furthermore, the decrease in TRDMT1 level makes human fibroblasts more susceptible to DNA damage and oxidative stress (Lewinska et al. 2018). Prior studies have also shown that perioperative use of Sevo for anesthesia can lead to varying degrees of stress response (Liu et al. 2012; Marana et al. 2013; Xu and Qian 2020). Consequently, we assumed that Sevo might affect DNMT1 expression in OC. In addition, TRDMT1 is a carcinogenic factor in gastric cancer and can contribute to its proliferation and metastasis (Sun et al. 2021). Importantly, TRDMT1 expression is augmented in OC and is a potential tumor-promoting factor for OC (Muranevich et al. 1988), but the exact role of TRDMT1 in OC remains elusive. Initially, TRDMT1 is considered a DNA methylation enzyme (Hermann et al. 2003), while it is a 5-methylcytosine (m5C) RNA methyltransferase. RNA m5C modification, one of the leading ways of post-transcriptional RNA modification, affects stability, maturation, and messenger RNA (mRNA) molecule translation, and is implicated in physiological and pathological processes, including stress response, carcinogenesis, and tumor cell migration (Guo et al. 2021). TRDMT1 is primarily responsible for promoting tRNA stability and protein synthesis by acting as m5C-modified "Writers" to modulate RNA m5C methylation (Goll et al. 2006; Tuorto et al. 2012). Recent data suggest that TRDMT1 is engaged in the m5C modification of tRNA and may boost mRNA methylation (Chen et al. 2020; Squires et al. 2012). For instance, TRDMT1 deletion afflicts the m5C modification of mRNA, and TRDMT1 knockdown can induce an reduction in the m5C methylation level of UGP2 mRNA (Xue et al. 2019), indicating the potential regulatory effect of TRDMT1 on mRNA m5C modification.

Adenomatous polyposis coli (APC) functions as a crucial tumor suppressor implicated in modulating tumor cell cycle, migration, apoptosis, invasion and proliferation (Fang and Svitkina 2022; Noe et al. 2021). The depletion of TRDMT1 in HEK293 cells can noticeably up-regulate the mRNA level of APC, which may be correlated to mRNA m5C modification (Xue et al. 2019). β-catenin protein is over-activated in OC and influences cancer cell metastasis, proliferation, stem cell stemness maintenance, and drug resistance (Nguyen et al. 2019; Shang et al. 2017). Furthermore, β-catenin is negatively regulated by APC to uphold cellular homeostasis (Ranes et al. 2021). Thus, we hypothesized that APC might be inhibited by TRDMT1 through mRNA m5C methylation modification. However, it is not clear whether TRDMT1 inhibits APC expression and activates the β-catenin pathway through m5C modification. Considering the connection of Sevo, TRDMT1, and cell phenotypes in OC, this research aims to investigate the

mechanism of Sevo modulating malignant behaviors, with a specific focus on the TRDMT1/m5C/APC/β-catenin axis.

Materials and methods

Ethics statement

All animal experiments were approved by the ethics committee of The Third Bethune Hospital of Jilin University. Significant attempts were made to reduce the quantity of animals and alleviate their suffering.

Cell culture

Human OC cell lines OVCAR3 and SKOV3 were sourced from American Type Culture Collection (Manassas, VA, USA), and appraised by Short Tandem Repeat to verify the purity and absence of contamination. Cell culture was conducted in Roswell Park Memorial Institute-1640 medium (Sigma-Aldrich, St. Louis, MO, USA) comprising 100 U/mL penicillin and streptomycin (Sigma-Aldrich) and 10% fetal bovine serum (FBS) in a 5% CO_2 incubator (Thermo Scientific, Rockford, IL, USA) at 37 °C.

Effect of Sevo on OC cell viability

Logarithmically growing OVCAR3 and SKOV3 cells (100 μL, 5×10^3/well) were introduced into 96-well plates and exposed to 3.6% Sevo (Hengrui Pharmaceutical Co., Ltd., Shanghai, China) for 0, 0.5, 1, 2, 4, 8, 12 and 24 h. According to the instructions and usage of Sevo, the concentration of Sevo for general anesthesia induction was 2.5–4.5%, and the maintaining anesthesia concentration was below 4%. As previously described (Ishikawa et al. 2021; Iwasaki et al. 2016), 3.6% Sevo treatment can strengthen the proliferation and malignant behaviors of ovarian cancer cells. Hence, we chose 3.6% Sevo as the research concentration. After exposure to Sevo, cells were subjected to 48 h of culture under normal conditions. Next, cell relative viability was evaluated by 3-(4,5-dimethylthiazol-2-yl)-2,5-diphenyltetrazolium bromide (MTT) assay. The treated OC cells were collected, with culture media removed. Afterward, cells were rinsed with phosphate-buffered saline (PBS) 2–3 times, mixed with 100 μL of culture medium comprising 0.5% MTT solution (M1025, Solarbio, Beijing, China), before being cultured for 4 h. Following the elimination of the supernatants, cells were treated with 100 μL/well of dimethyl sulphoxide (DMSO) and slowly shaken on a shaker for 15 min. The optical density (OD) values at 570 nm were determined by a microplate reader (Thermo Scientific). The cell relative viability was denoted as a percentage (%). The group treated with Sevo for 0 h was set as control (100%).

Cell grouping and treatment

The 100 μL logarithmically growing OVCAR3 and SKOV3 cells were inoculated (5×10^3/well) onto 96-well plates and grouped as below: (1) the Blank group, OC cells underwent 48 h of culture; (2) the Sevo group, OC cells were exposed to 3.6% Sevo for 2 h and then cultured under normal circumstances for 48 h; (3) the Sevo + si-NC group and the Sevo + si-TRDMT1 group, after transfection of the small-interfering (si)-TRDMT1 or si-negative control (NC), OC cells were subjected to 3.6% Sevo exposure for 2 h and subsequent 48-h cultivation under normal conditions; (4) the Sevo + si-TRDMT1 + sh-NC and Sevo + si-TRDMT1 + short hairpin (sh)-APC groups, OC cells were exposed to 3.6% Sevo for 2 h, and then cultured under normal conditions for 48 h following co-transfection of si-TRDMT1 and sh-NC or sh-APC; (5) the Sevo + sh-NC and Sevo + sh-β-catenin groups, OC cells were manipulated with si-β-catenin or sh-NC, followed by 2-h exposure to 3.6% Sevo and 48-h culture under standard conditions. The steps of the transfection were as follows: cells were introduced onto the 6-well plate. Once the cell confluence arrived 80%, si-NC, si-TRDMT, sh-NC, sh-APC, and sh-β-catenin were delivered into cells utilizing Lipofectamine® 3000 (L3000-015, Invitrogen, Carlsbad, CA, USA), and the transfection amount of these plasmids (GenePharma, Suzhou, Jiangsu, China) was 2 μg/well. The target sequences of the interference plasmids were: si-TRDMT1: 5'-CCAAAGTCATTG CTGCGATAT-3'; sh-APC: 5-GCCAACAAAGTC ATCACGTAA-3; and sh-β-catenin: 5'-GAGGAG TTCCTGCGCACCTAT-3'. Following 48-h transfection, the expression patterns of TRDMT1, APC and β-catenin were measured by western blot and reverse transcription quantitative polymerase chain reaction (RT-qPCR) to ascertain the transfection efficiency.

Thereafter, the biological behavior indexes of OC cells were assessed.

Cell counting kit-8 (CCK-8) assay

OC cell proliferative activity was evaluated using CCK-8 kit (KTA1020, Abbkine Scientific Co., Ltd., Wuhan, Hubei, China). Cells at the exponential phase were plated into 96-well plates and treated in distinct groups. After culture for 12, 24, and 48 h, cells were supplemented with CCK-8 solution (10 μL/well) for a 2-h incubation at 37 °C. Then, the OD value was ascertained at 450 nm with the Thermo Scientific microplate reader (Thermo Scientific). The test was repeated thrice, with the result average value acquired. Cell doubling time was counted based on the following formula (Colosimo et al. 2013): TD = t × lg2/(lgNt—lgN0) (TD: the doubling time of cells, t: the incubation duration, Nt: the OD value at t hour of incubation, and N0: the OD value after seeding).

Colony formation assay

The cell proliferative capacity was assessed by colony formation assay. Differently-treated OC cells (OVCAR3 and SKOV3) were gathered and detached into single cells by trypsin. Approximately 700 single cells were seeded into 6-well plates and cultivated at 37 °C for 10–14 days until colony formation was visible. Cells underwent 30-min fixation with 4% paraformaldehyde, with PBS washing followed. Next, cells were subjected to crystal violet (V5265, Sigma-Aldrich) staining for 20 min, then rinsed with PBS thrice, dried, observed and photographed, with the quantity of cell clones per well counted. Each group was set up with three duplicate wells. The results were expressed as average values.

Flow cytometry

The Cell Cycle and Apoptosis Analysis Kit [propidium iodide (PI) staining] (HY-K1071, MedChemExpress, Monmouth Junction, NJ, USA) was utilized to confirm the cell cycle distribution and apoptotic rate. In brief, OVCAR3 and SKOV3 cells after different treatments were gathered into 1.5-mL centrifuge tubes, then cleaned twice with pre-cooled PBS and immobilized with 70% pre-cooled ethanol at 4 °C all night. Thereafter, cells were cleaned and resuspended in pre-cooled PBS and cultured in the presence of RNase and PI (each 10 mg/mL) for 30 min at 37 °C without light to assess cell cycle. Alternatively, cells were cultivated with 5 μL PI solution and 10 μL Annexin V-fluorescein isothiocyanate solution at 37 °C without light for 30 min to evaluate apoptosis. After staining, cell percentages in varying cell cycles (G0/G1, S, and G2/M) (%) or apoptotic rate (%) were analyzed by the flow cytometer (Becton, Dickinson and Company, Franklin Lakes, NJ, USA) and Flowjo V10 software (FlowJo, Seattle, WA, US). The experiment was duplicated thrice, and the results were averaged.

Transwell assay

Transwell assay was implemented to test cell invasion and migration. Simply put, cells with different treatments underwent PBS cleaning twice and resuspension in a serum-free medium and were counted. After cell concentration was adjusted, 100 μL cell suspension (1×10^4) was seeded onto the upper chamber of the Transwell chamber (Corning Incorporated, Corning, NY, USA), while 600 μL medium supplemented with 10% FBS was placed onto the lower chamber; with a layer of matrigel (60 μL, Corning) evenly spread at the bottom, middle apical chambers (no matrigel was spread when detecting cell migration. After 24 h of cell incubation at 37 °C, the chamber was taken out before PBS washing two times. Following this, the chamber was immobilized for 30 min using methanol at 37 °C and dyed with 0.5% crystal violet (G1065, Solarbio) for 20 min. Cells at the apical chamber bottom that did not invade or migrate were erased. The chamber was thereafter examined and imaged under an inverted microscope (CKX53, OLYMPUS, Tokyo, Japan). Finally, 5 non-overlapping fields of view were selected stochastically to conduct cell invasion or migration counts. The obtained results were averaged, and each group of tests was completed repeatedly thrice.

Cell scratch test

Cell scratch test was executed to evaluate the OC cell migratory capacity. OC cells (OVCAR3 and SKOV3) after different treatments were collected, and they were plated into 6-well plates at 2×10^5 cells each

well and fostered for 24 h at 37 °C with 5% CO_2. A pipette tip (200 µL) was used to draw a line perpendicular to the cell surface, and the cells were cultured for 24 h afterward. The scratch width was tested by the inverted microscope (OLYMPUS) at 0 and 24 h subsequent to scratching, and images were obtained. The scratch healing rate (%) was computed to test cell migratory capability.

RT-qPCR

Isolation of total cellular RNA from differently-treated OC cells was executed via the TRIzol reagent (15596–018, Thermo Scientific), with its concentration and purity determined using a NanoDrop2000C Ultra-Micro Spectrophotometer (Thermo Scientific). The reverse transcription kit (GeneCopoeia, Rockville, MD, USA) was utilized for reverse transcription to obtain complementary DNA. Later, qPCR was implemented on the 7500 Real-Time PCR system (Applied Biosystems, Carlsbad, CA, USA) under the following conditions: 10-min pre-denaturation at 95 °C, and 40 cycles of 10-s denaturation at 95 °C, 10-s annealing at 60 °C and 20-s extension at 72 °C. GAPDH was deemed as the internal reference gene. Using the $2^{-\Delta\Delta Ct}$ technique, the relative gene expression was confirmed (Schmittgen and Livak 2008). The synthesis of all primers was provided by Tsingke Biotech (Beijing, China), as displayed in Table 1.

Bioinformatics analysis

The NCBI database (https://www.ncbi.nlm.nih.gov/) was utilized to search for the APC mRNA sequence. The Human APC gene mRNA number is "M74088.1". The potential m5C methylation modification sites on APC mRNA were predicted utilizing the iRNA m5C database (http://lin-group.cn/server/iRNA-m5C/service.html) (Li et al. 2018). The potential m5C methylation sites located near the start site of the APC mRNA CDS 5' end upstream were named Site1, and the sites situated near the end of the 3' end were designated Site2.

Methylated RNA immunoprecipitation (MeRIP) assay

As mentioned earlier (Luo et al. 2022), the level of m5C methylation on APC mRNA was examined using the m5C MeRIP kit (GS-ET-003, Yunsui Biotechnology Co., Ltd., Shanghai, China). In the beginning, total RNA was gained from OC cells that had been subjected to different treatments. Subsequently, the extracted RNA was fragmented into fragments of 100–200 nt size using the RNA fragmentation reagent. Next, immunoprecipitation of the fragmented RNA was implemented using m5C, protein A/G magnetic beads, and immunoglobulin G (IgG) antibody. Also, immunoprecipitated RNA was competitively eluted using 5-methylcytosine hydrochloride (M6751, Sigma-Aldrich). The RNA was resuspended, before analysis of mRNA-containing m5C enrichment by RT-qPCR. Lastly, the $2^{-\Delta\Delta Ct}$ method was employed to confirm the m5C methylation level of APC mRNA. The primers for gauging APC mRNA Site1 m5C methylation were 5'-CTCGTACTTCTGGCCACT G-3' and 5'-TCAGTGCCTCAACTTGCTTT-3'; the primers for Site2 were 5'-GGGTTTTTTTGTTCT GGAAGCCA-3' and 5'-AAGTTGGGGATGGGT GCTACT-3'.

Actinomycin D assay

APC mRNA stability was valued by actinomycin D assay as previously described (Hu et al. 2001). Differently-treated cells were subjected to 5 µg/mL actinomycin D (114,666, Sigma-Aldrich) treatment for 0, 2, 4, and 6 h, in a bid to impede mRNA transcription. Moreover, the impact of m5C methylation modification on APC mRNA stability was estimated by measuring the relative expression of APC mRNA using RT-qPCR.

Table 1 Primer sequences in RT-qPCR

Gene	Forward 5'-3'	Reverse 5'-3'
TRDMT1	TCTCCAACCTCTCTTGGCATTC	GGGAACTCCATCAGTACCTGACCA
APC	AGCACAGCGAAGAATAGCCA	AGGTGCAGAGTGTGTGCTAC
GAPDH	TGAGAACGGGAAGCTTGTCA	CCCTGCAAATGAGCCCCA

Fluorescent In Situ Hybridization (FISH) and immunofluorescence double staining assays

Co-localization of APC mRNA with TRDMT1 protein was confirmed by FISH and immunofluorescence double staining assays. At first, the cell slides of OVCAR3 and SKOV3 cells were put into preparation, fixated with 4% paraformaldehyde (158,127, Sigma-Aldrich) at 4 °C, and blended with 0.1% Triton-X-100 (X100, Sigma-Aldrich) to break the membranes. The slides were added with 5 μL Cyanine3-labeled APC mRNA nucleic acid probe hybridization solution (Ribobio Biotechnology Co., Ltd., Guangzhou, Guangdong, China), before overnight cultivation at room temperature in darkness. Following PBS rinsing, cell slides were closed with 3% bovine serum albumin (BSA), interacted with anti-TRDMT1 primary antibody (4 μg/mL, ab244461, Abcam, Cambridge, UK) all night at 4 °C away from light, and co-incubated for 1 h with Alexa Fluor® 488-coupled IgG (1:1000, ab150077, Abcam) at room temperature in the lack of light. Afterward, cell nuclei were dyed using 4',6-diamidino-2-phenylindole (DAPI) (ab285390, Abcam) and cultured at room temperature, shielded from light, for 5 min. Eventually, the observation of the co-localization of APC mRNA with TRDMT1 protein was conducted using an inverted fluorescent microscope (DMI3000B, Leica, Solms, Germany).

RNA pull down assay

APC mRNA pcDNA3.1 overexpression plasmid (Genecreate Bioengineering Co., Ltd, Wuhan, Hubei, China) was constructed, and biotin (Bio)-labeled APC mRNA sense (Bio-APC mRNA sense) and anti-sense (Bio-APC mRNA antisense) sequences were synthesized in vitro by T7 RNA polymerase and qPCR assays. Bio-marked RNA interacted with cell protein lysates to form RNA–protein complexes. The protein complexes were precipitated and eluted via the Pierce™ magnetic RNA–protein Pull-Down kit (20,164, Thermo Scientific), as per the provided protocols. Ultimately, western blot assay was implemented to define the TRDMT1 level enriched by Bio-APC mRNA sense and Bio-APC mRNA antisense to test whether APC mRNA interacted with TRDMT1 protein.

Co-immunoprecipitation (Co-IP) assay

The extraction of total protein was performed by introducing IP cell lysate (R21241, Yuanye Biotechnology Co., Ltd., Shanghai, China). Next, the bicinchoninic acid (BCA) kit (PA115-01, TIANGEN, Beijing, China) was applied to determine the protein content. The total protein (50 μg) was incubated with 2 μg of anti-β-catenin (ab265591, Abcam) or anti-IgG (ab6715, Abcam) all night at 4 °C, and grown with 10 μL proteinA/G magnetic beads (abs9649, Ambition Biotechnology Co., Ltd., Beijing, China) for 2 h at 4 °C. Following the IP reaction, the level of APC that had been immunoprecipitated by β-catenin was examined by western blot. A sample of protein lysate without IP treatment was considered as Input.

Cellular immunofluorescence

Cell fixation was carried out for 30 min utilizing 4% paraformaldehyde (158,127, Sigma-Aldrich) prior to 5-min cell treatment with a membrane-breaking reagent, specifically 0.1% Triton X-100 (Sigma-Aldrich). Afterward, cells were closed using 5% BSA for 45 min, with the BSA solution aspirated off. Cells then received overnight incubation with a primary antibody, anti-β-catenin (1:250, ab265591, Abcam) at 4 °C. After being rinsed by PBS, cells were cultivated and avoided light for 45 min at room temperature with IgG H&L Alexa Fluor® 594 (1:200, ab150120, Abcam). Cells received PBS cleaning again, and the nuclei underwent DAPI staining (ab285390, Abcam), followed by glycerol sealing subsequent to PBS washing. The nuclear translocation of β-catenin was viewed under an inverted fluorescence microscope (DMI3000B, Leica).

Animal feeding and xenograft tumor models

BALB/c nude mice ($n = 48$, 5–6 weeks old, weighing 21 ± 2 g), procured from Jilin Qianhe Model Biotechnology Co., Ltd. (Changchun, Jilin, China), were reared under the conditions of 26 ± 1 °C temperature, 50–60% air humidity, and a 12-h light/dark cycle in a specific pathogen-free circumstance and with freely available water and food. Following 1-week acclimatization, the nude mice were assigned to 4 groups at random, ensuring 6 nude/per group with tumor formation ($n = 6$). Animal grouping processing was as

follows: the Control group, nude mice were subcutaneously administered with cells in the logarithmical growth to generate a xenograft model; the Sevo group, the nude mouse xenograft model was developed via hypodermic injection of 3.6% Sevo-pretreated cells for 2 h into nude mice; the Sevo + KD-NC group and the Sevo + KD-TRDMT1 group, cells were delivered with lentivirus-packed TRDMT1 interference plasmid or NC plasmid, pretreated with 3.6% Sevo for 2 h, and injected hypodermically into nude mice to develop the xenograft tumor model.

In a nutshell, the lentivirus stable cell screening method could be explained as follows: OVCAR3/SKOV3 cells were initially treated with lentivirus loaded with si-TRDMT1 plasmid or si-NC plasmid (containing puromycin resistance gene), then screened by puromycin (5 μg/mL) for 48 h, and amplified by adding the medium containing 1 μg/mL puromycin. TRDMT1 low-expressing stably-transformed cell lines were obtained when RT-qPCR assay testified stable TRDMT1 low-expression in the cells. Tumor volume was measured weekly. Mice were euthanized with the administration of an excessive dosage of 2% pentobarbital sodium (200 mg/kg) following the final assessment of tumor volume on day 28. Tumor tissues were taken out, imaged and weighed, with sectional tumor tissues fixated by means of 4% paraformaldehyde for 12 h. Paraffin embedding was made to make sections of 5 μm thickness. The rest tumor tissues were made into tissue homogenates, followed by determinations of TRDMT1, APC, and β-catenin protein levels by western blot.

Immunohistochemistry

Paraffin sections of tumor tissues (5 μm) were conventionally dewaxed to water, before being incubated for 10 min with 3% H_2O_2 (R20847, Yuanye Bio-Technology, Shanghai, China) at room temperature to eradicate endogenous peroxidase activity. Next, antigen retrieval was executed via microwave heating in citric acid buffer (0.01 M, pH 6.0). After cooling, sections were sealed at room temperature with 10% goat serum (G9023-10ML, Sigma-Aldrich) for 10 min, followed by overnight interaction with primary antibody anti-Ki-67 (1:250, Abcam) at 4 °C and 3 PBS rinses, and then 30-min interaction with Bio-labeled anti-IgG (1:2000, ab207995) at room temperature. Subsequently, sections were stained with freshly prepared 3,3'-diaminobenzidine (R21317, Yuanye Bio-Technology), re-stained with hematoxylin (B25380-20 mg, Yuanye Bio-Technology), differentiated with 1% hydrochloric acid ethanol, dehydrated, and blocked with neutral resin, and finally viewed and imaged under an optical microscope (OLYMPUS). Image J software (NIH, Bethesda, MD, USA) was processed for counting Ki-67 positive cell percentages (%).

Western blot assay

The animal tissue and cell total protein extraction kit (column method) (BC3790, Solarbio) was applied to separate the total protein out of cells or

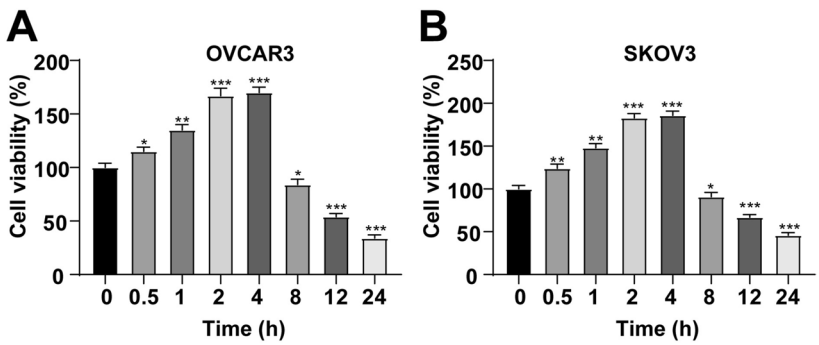

Fig. 1 Effects of Sevo treatment on OC cell viability. OC cell lines OVCAR3 and SKOV3 cells were treated with 3.6% Sevo for 0, 0.5, 1, 2, 4, 8, 12 and 24 h, and then cultured under normal conditions for 48 h. **A**-**B**: MTT assay to assess the relative cell viability. Cell experiments were repeated independently three times, and the data were expressed as mean ± SD. The group treated with Sevo for 0 h was set as the Control group. Independent sample *t*-test was used for comparisons between two groups, and one-way ANOVA was for comparisons among multiple groups. * $p < 0.05$, ** $p < 0.01$, *** $p < 0.001$

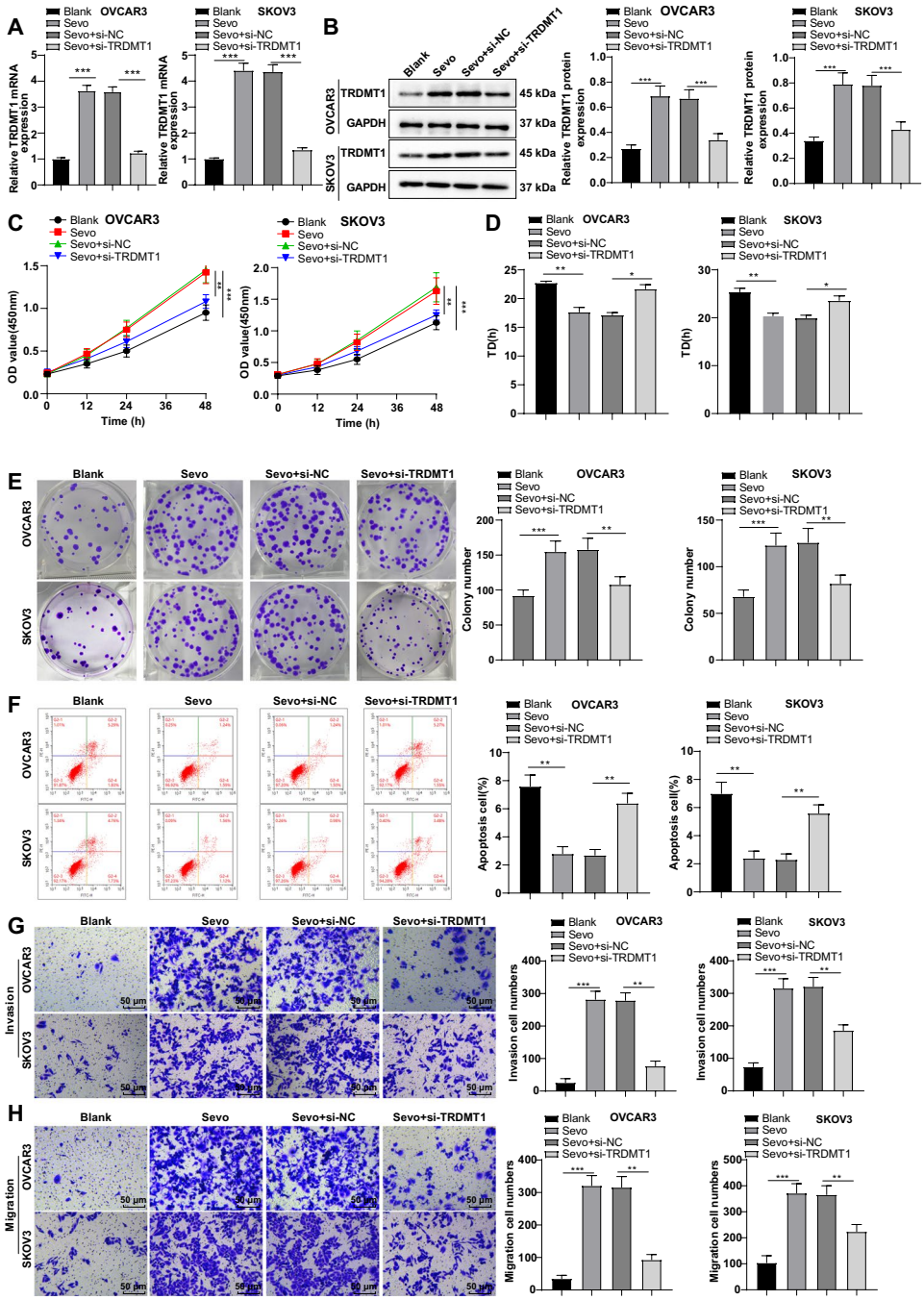

Fig. 2 Sevo promoted OC cell proliferation, invasion, and migration and inhibited apoptosis by up-regulating TRDMT1. OC cell lines OVCAR3 and SKOV3 were treated with 3.6% Sevo for 2 h and simultaneously transfected with interference plasmid of TRDMT1 to knock down TRDMT1 expression. **A**-**B**: The mRNA and protein levels of TRDMT1 determined by RT-qPCR and western blot assays; **C**: Cell proliferation evaluated by CCK-8 assay; **D**: Bar chart analysis on the differences in cell doubling time among different groups; **E**: OC cell proliferative ability assessed by colony formation assay; **F**: Cell apoptotic rate assessed by flow cytometry; **G**-**H**: Cell invasion and migration assessed by Transwell assay; **I**: Cell scratch assay was used to assess the migratory ability of OC cells. Repeated cell experiments were performed independently three times and the data were expressed as mean ± SD. One-way ANOVA was employed for comparisons among multiple groups. * $p < 0.05$, ** $p < 0.01$, *** $p < 0.001$

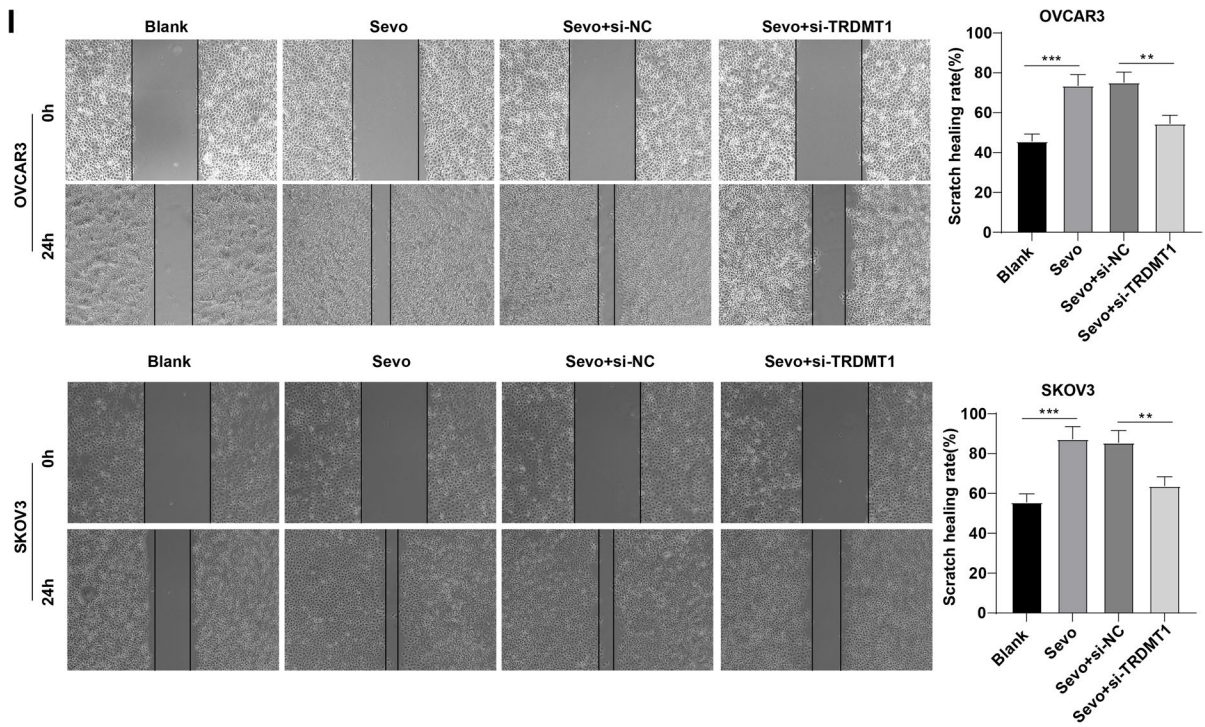

Fig. 2 (continued)

tumor tissues, or the nucleoprotein extraction kit (R0050, Solarbio) was utilized to extract nucleoprotein. BCA protein quantification kit (PA115-01, TIANGEN) was applied to measure protein concentration. The samples were boiled for 10 min to fully denature the protein, which was separated by 8% sodium dodecyl sulfate–polyacrylamide gel electrophoresis, with 20 μg total protein loaded each well. After separation, the protein samples were moved onto polyvinylidene fluoride membranes by the wet electrotransfer method and closed with tris-buffered saline-tween (TBST) comprising 5% skim milk at room temperature for 2 h. Afterward, the samples were mixed with the following primary antibodies for incubation all night at 4 °C: GAPDH (1:10,000, ab181602), TRDMT1 (1:1000, ab308120, Abcam), cyclin D1 (1:25, ab16663), APC (1:5000, ab40778), β-catenin (1:1000, ab265591), C-myc (1:1000, ab32072), and Histone H3 (1:1000, ab1791). The samples were subsequently cleaned thrice with TBST and cultured in the presence of Goat Anti-Rabbit IgG H&L secondary antibody (1:20,000, ab97051) at 37 °C for 1 h. After being cleaned three times with TBST again, the samples received color development and image collection with an enhanced chemiluminescence working solution (P0018M, Beyotime, Shanghai, China). The bands were quantitatively analyzed using Image J (NIH). GAPDH was deemed as the internal reference of total protein; Histone H3 was presented as the internal reference of nuclear protein.

Statistical analysis

SPSS22.0 (IBM, Armonk, New York, USA) and GraphPad Prism 9.0 (GraphPad Software, Inc., San Diego, CA, USA) were employed for data handling, analysis, and mapping. The normal distribution was tested by the Shapiro–Wilk test. Cell tests were independently replicated thrice, with data denoted as mean ± standard deviation (SD), and tested between groups using the *t*-test. Multi-group comparisons were made using one-way analysis of variance (ANOVA). p was a bilateral test, with a $p < 0.05$ representing significant differences.

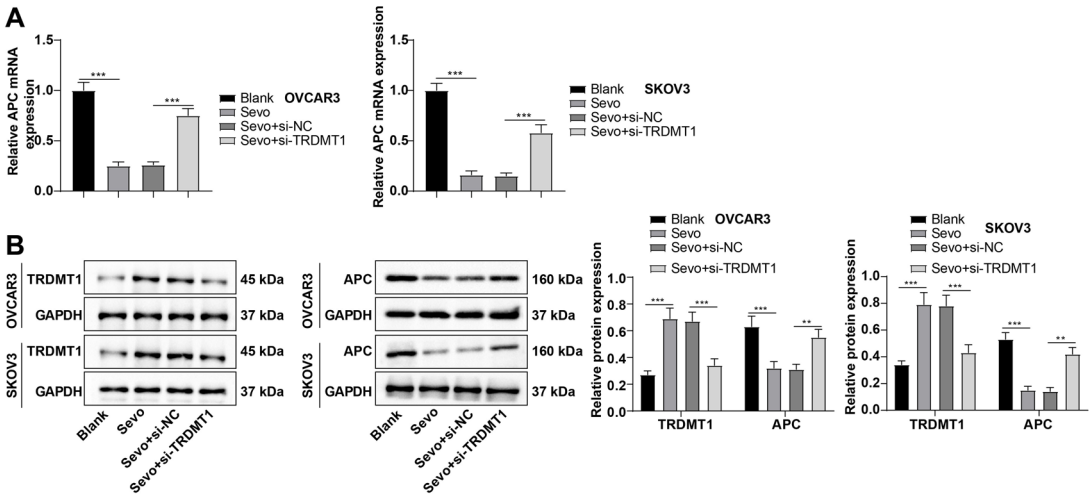

C

Sequence	C position	Modification
>M74088.1 HumAn APC Gene mRNA, CompleTe Cds	23	Yes
>M74088.1 HumAn APC Gene mRNA, CompleTe Cds	26	Yes
>M74088.1 HumAn APC Gene mRNA, CompleTe Cds	29	Yes
>M74088.1 HumAn APC Gene mRNA, CompleTe Cds	32	Yes
>M74088.1 HumAn APC Gene mRNA, CompleTe Cds	8920	Yes
>M74088.1 HumAn APC Gene mRNA, CompleTe Cds	8925	Yes
>M74088.1 HumAn APC Gene mRNA, CompleTe Cds	8929	Yes
>M74088.1 HumAn APC Gene mRNA, CompleTe Cds	8932	Yes

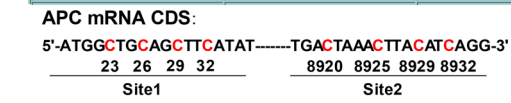

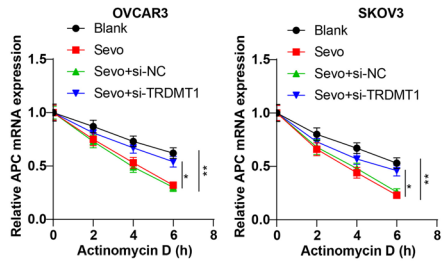

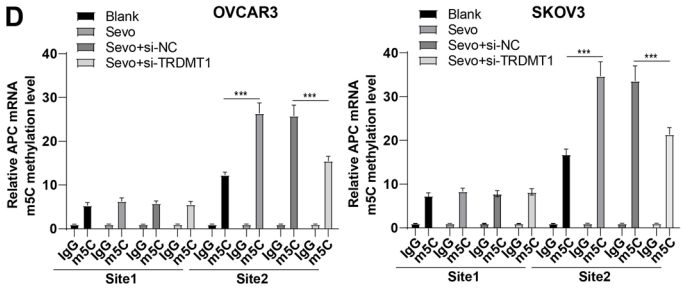

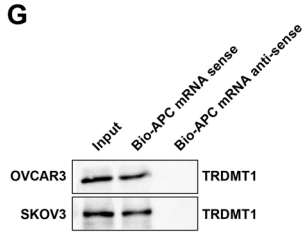

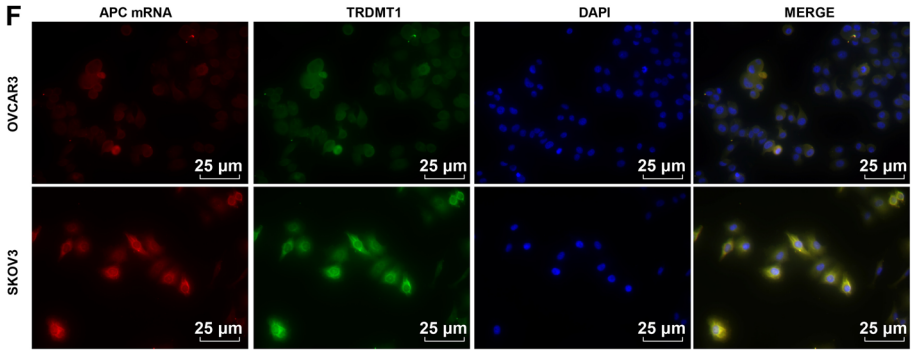

◂**Fig. 3** Sevo promoted m5C modification of APC mRNA and suppressed its expression by up-regulating TRDMT1. **A**: The APC mRNA level measured by RT-qPCR; **B**: The protein levels of TRDMT1 and APC assessed by western blot; **C**: The potential m5C methylation sites in APC mRNA predicted by the bioinformatics website database iRNA m5C (http://lin-group.cn/server/iRNA-m5C/service.html); **D**: m5C methylation modification levels near APC mRNA Site1 and Site2 detected by the m5C meRIP-qPCR assay; **E**: Stability of APC mRNA tested by actinomycin D assay; **F**: Cellular localization of APC mRNA and TRDMT1 protein in OC cells observed by FISH and immunofluorescence assays; **G**: The binding between APC mRNA and TRDMT1 in OC cells examined by RNA pull down assay. Repeated cell experiments were conducted separately three times and the data were expressed as mean ± SD. One-way ANOVA was applied for comparisons among multiple groups. * $p < 0.05$, ** $p < 0.01$, *** $p < 0.001$

Results

Effects of Sevo on OC cell viability

To study the impact of Sevo on OC cell viability, we treated cells with 3.6% Sevo for 0, 0.5, 1, 2, 4, 8, 12, and 24 h and continued to cultured cells under standard conditions for another 48 h. MTT assay showed that Sevo pretreatment for 0.5–4 h could fortify OC cell proliferative activity, and cell viability after 2 and 4 h was the highest and kept stable, while pretreatment for 8–24 h attenuated the proliferative activity (Fig. 1A-B, all $p < 0.05$). Consequently, a treatment duration of 2 h was chosen for the administration of Sevo in the following experimental trials.

Sevo facilitated OC cell proliferation, invasion and migration and repressed apoptosis by up-regulating TRDMT1

A previous study has revealed that increased TRDMT1 expression in OC is associated with cisplatin resistance (Zhu et al. 2021). To further probe whether short-term stimulation with Sevo affected the biological behaviors of OC cells by impacting TRDMT1 expression, we used 3.6% Sevo to treat OC cells for 2 h while delivering them with interference plasmids to regulate TRDMT1 in OC cells. Sevo up-regulated the expression of TRDMT1, while the expression was subdued after transfection with interference plasmid (Fig. 2A-B, all $p < 0.001$). Besides, Sevo treatment accelerated the proliferation of OC cells and reduced cell doubling time, while knockdown of TRDMT1 expression partially inhibited their proliferation and augmented cell doubling time (Fig. 2C-D, all $p < 0.001$). Also, Sevo treatment could potentiate the proliferation of OC cells, while TRDMT1 knockdown curbed cell proliferation (Fig. 2E, all $p < 0.01$). Sevo treatment could inhibit the apoptosis of OC cells, while lowly-expressed TRDMT1 raised the apoptotic rate (Fig. 2F, all $p < 0.01$). Next, Sevo hastened OC cell invasiveness and migration, while the invasive and migratory abilities were weakened after TRDMT1 silencing (Fig. 2G-H, all $p < 0.01$). Besides, Sevo could heighten OC cell migration, whereas TRDMT1 knockdown impeded the migration (Fig. 2I, all $p < 0.01$). These results revealed that Sevo could reinforce OC cell proliferation, invasion, and migration and curtail apoptosis by up-regulating TRDMT1.

Sevo up-regulated TRDMT1 to promote m5C modification of APC mRNA and suppress its expression

Subsequently, it was imperative to conduct a more comprehensive exploration into the downstream mechanism of TRDMT1 regulation. APC is one of the critical tumor suppressor factors that exert regulatory control on various cellular processes correlated with tumorigenesis, including cell proliferation, apoptosis, invasiveness, and migration (Fang and Svitkina 2022; Noe et al. 2021). Meanwhile, an existing study has shown that TRDMT1 may control the mRNA level of APC by influencing the m5C modification of RNA (Xue et al. 2019). As a result, we speculated that TRDMT1 might impact OC cell biological behaviors by modulating APC expression. Sevo inhibited APC expression in OC cells, while its inhibition was partially alleviated following TRDMT1 knockout (Fig. 3A-B, all $p < 0.01$). The APC mRNA CDS sequence was derived from the NCBI database, and the potential APC mRNA m5C modification sites were predicted via the bioinformatics website based on the random forest algorithm. There were multiple potential m5C modification sites close to the 5'-end translation initiation site (Site1) and the 3'-end (Site2) of APC mRNA (Fig. 3C). Concerning the results of the m5C meRIP-qPCR assay, Sevo treatment raised the m5C methylation level near Site2 of APC mRNA, whereas the level dropped after knocking down TRDMT1 (Fig. 3D, all $p < 0.001$), but there

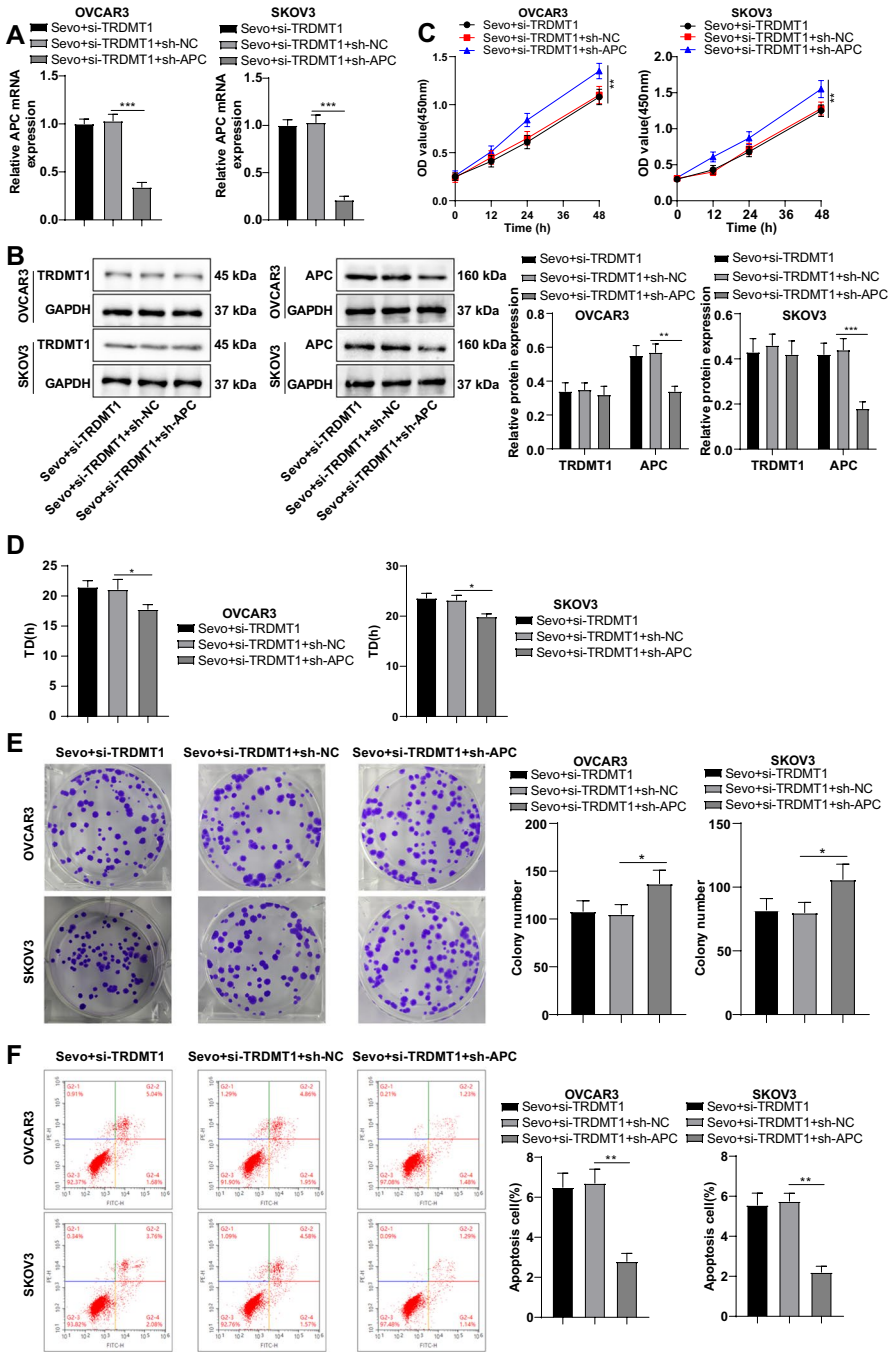

Fig. 4 Sevo boosted OC cell proliferation, invasion, and metastasis and hindered apoptosis through TRDMT1 regulating APC expression. The expression levels of TRDMT1 and APC were down-regulated by simultaneous transfection of TRDMT1 and APC interference plasmids in OC cells, and the cells were then subjected to Sevo treatment. **A**-**B**: RT-qPCR and western blot experiments to determine mRNA and protein levels of TRDMT1; **C**: CCK-8 assay to assess cell proliferation; **D**: The difference in cell doubling time between each group was analyzed by bar chart; **E**: The proliferative ability of OC cells was assessed by cell colony assay; **F**: Flow cytometry to evaluate cell apoptotic rate; **G**-**H**: Transwell assay to evaluate cell invasion and migration; **I**: Cell scratch assay to evaluate the migratory ability of OC cells. Repeated cell experiments were performed independently three times and the data were expressed as mean ± SD. One-way ANOVA was adopted for comparisons among multiple groups. * $p < 0.05$, ** $p < 0.01$, *** $p < 0.001$

was no prominent change in m5C methylation level near the APC mRNA Site1 site (Fig. 3D, all $p > 0.05$).

We further evaluated the half-life changes of APC mRNA in OC cells by actinomycin D assay and clarified that Sevo enhanced the degradation of APC mRNA, whereas TRDMT1 silencing reinforced the stabilization of APC mRNA (Fig. 3E, all $p < 0.05$), indicating that Sevo might augment the m5C methylation modification of APC mRNA via the upregulation of TRDMT1 expression, hence facilitating its degradation. Beyond that, we observed the co-localization of APC mRNA with TRDMT1 protein in the cytoplasm by FISH and immunofluorescence experiments (Fig. 3F).

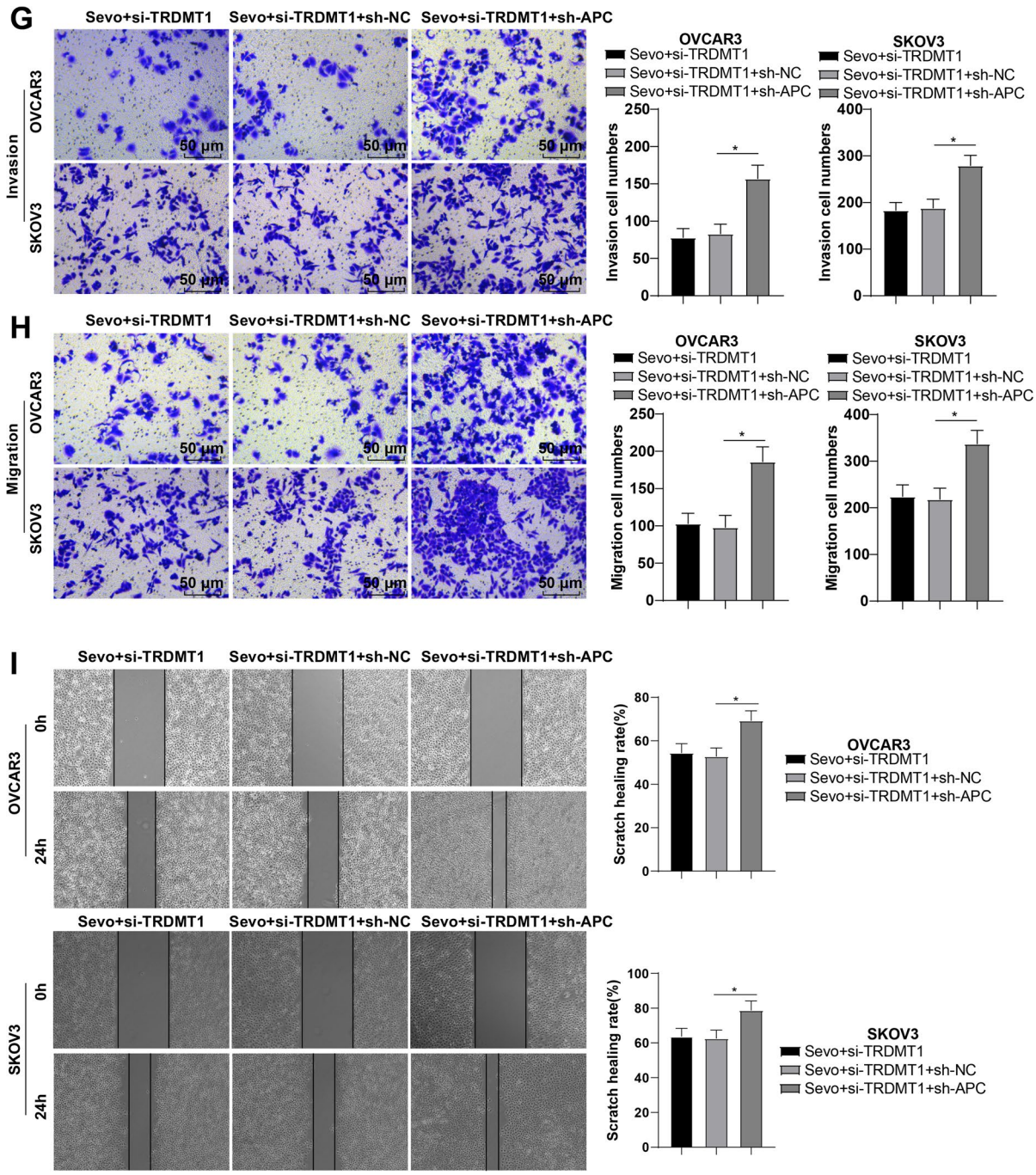

Fig. 4 (continued)

TRDMT1 was enriched in the Bio-APC mRNA sense (Fig. 3G), which further validated that TRDMT1 could bind to APC mRNA to regulate its m5C methylation modification to suppress APC expression.

Sevo boosted OC cell proliferation, invasion and metastasis and hindered apoptosis via TRDMT1/APC

In the quest to further plumb whether Sevo modulated OC cell biological behaviors via regulation of

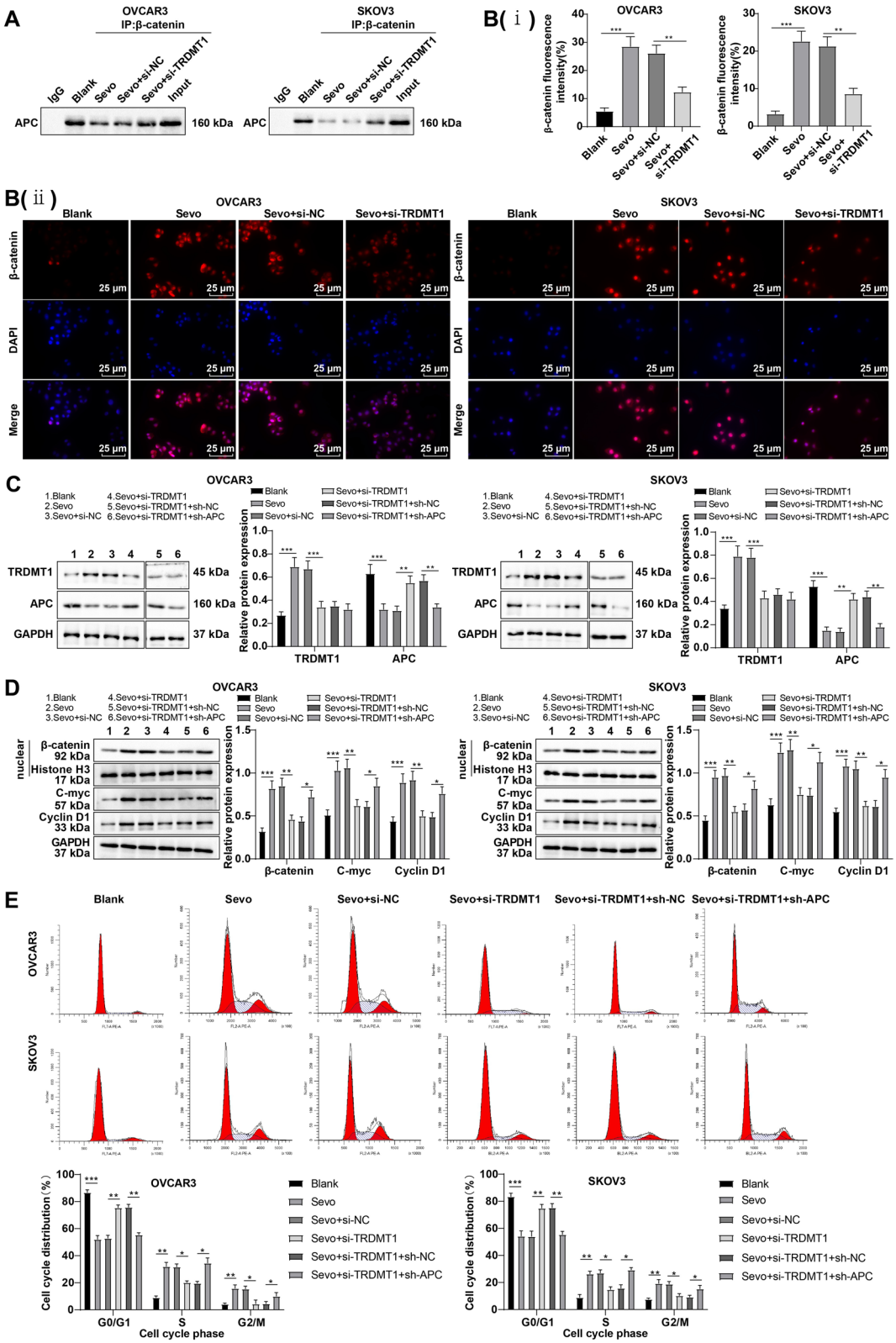
A
OVCAR3
IP:β-catenin
SKOV3
IP:β-catenin
IgG
Blank
Sevo
Sevo+si-NC
Sevo+si-TRDMT1
Input
APC
160 kDa
B(i)
OVCAR3
SKOV3
β-catenin fluorescence intensity(%)
Blank
Sevo
Sevo+si-NC
Sevo+ si-TRDMT1
B(ii)
OVCAR3
SKOV3
Blank
Sevo
Sevo+si-NC
Sevo+si-TRDMT1
β-catenin
DAPI
Merge
25 μm
C
OVCAR3
SKOV3
1.Blank
2.Sevo
3.Sevo+si-NC
4.Sevo+si-TRDMT1
5.Sevo+si-TRDMT1+sh-NC
6.Sevo+si-TRDMT1+sh-APC
Sevo+si-TRDMT1+sh-NC
Sevo+si-TRDMT1+sh-APC
TRDMT1
APC
GAPDH
45 kDa
160 kDa
37 kDa
Relative protein expression
D
OVCAR3
SKOV3
nuclear
β-catenin 92 kDa
Histone H3 17 kDa
C-myc 57 kDa
Cyclin D1 33 kDa
GAPDH 37 kDa
β-catenin
C-myc
Cyclin D1
E
Blank
Sevo
Sevo+si-NC
Sevo+si-TRDMT1
Sevo+si-TRDMT1+sh-NC
Sevo+si-TRDMT1+sh-APC
OVCAR3
SKOV3
Cell cycle distribution (%)
G0/G1
S
G2/M
Cell cycle phase

◂**Fig. 5** Sevo activated the β-catenin pathway through TRDMT1/APC to modulate cell cycle progression. **A**: CO-IP assay to detect the protein interaction between APC and β-catenin; **B**: The immunofluorescence assay to observe the nuclear translocation level of β-catenin; **C**-**D**: Western blot to determine the protein levels of TRDMT1, APC, nuclear β-catenin, C-myc, and Cyclin D1; **E**: Flow cytometry to examine cell cycle distribution. Repeated cell trials were performed independently thrice and the data were represented as mean ± SD. One-way ANOVA was adopted for comparisons among groups. * $p < 0.05$, ** $p < 0.01$, *** $p < 0.001$

APC expression through TRDMT1, we co-transfected OC cells with interference plasmids to down-regulate TRDMT1 and APC expression and treated cells with Sevo. RT-qPCR and western blot assays noted repressed APC expression (Fig. 4A-B, all $p < 0.01$), yet TRDMT1 expression did not change evidently, suggesting that TRDMT1 was not affected by APC expression (Fig. 4B, all $p > 0.05$). Furthermore, after APC knockdown, OC cell proliferation was increased (Fig. 4C, all $p < 0.01$), cell doubling time dropped (Fig. 4D, all $p < 0.05$), the number of cell colonies was increased (Fig. 4E, all $p < 0.05$), the apoptotic rate was diminished (Fig. 4F, all $p < 0.01$), cell invasion and migration were boosted (Fig. 4G-H, all $p < 0.05$), and cell scratch healing ability was weakened (Fig. 4I, all $p < 0.05$). These foregoing findings proved that Sevo encouraged the growth and metastasis of OC cells while suppressing apoptosis by modulating APC expression via TRDMT1.

Sevo activated the β-catenin pathway via TRDMT1/APC to modulate cell cycle progression

Available reports indicate that APC primarily exerts its biological activity by acting as a β-catenin pathway inhibitory factor, and β-catenin can control cell biological behaviors by modulating C-myc and Cyclin D1 (Nguyen et al. 2019; Shang et al. 2017; Ranes et al. 2021). Accordingly, we examined the putative hypothesis that Sevo afflicted the OC cell cycle by modulating the β-catenin pathway via TRDMT1/APC. Sevo treatment could retard the interaction of APC with β-catenin, while TRDMT1 knockout could encourage the interaction (Fig. 5A). Sevo assisted β-catenin into the nucleus, while lowly-expressed TRDMT1 limited its nuclear level (Fig. 5B, all $p < 0.01$). Furthermore, Sevo was capable of activating the β-catenin pathway and increasing levels of Cyclin D1, C-myc and β-catenin. Following knockdown of TRDMT1, the β-catenin pathway was curtailed, whereas the β-catenin pathway was reactivated after APC was simultaneously silenced; besides, APC silencing had no significant effect on TRDMT1 expression, confirming that APC was at downstream of TRDMT1 (Fig. 5C-D, all $p < 0.05$). Sevo could boost OC cell cycle progression, which was manifested by lessened numbers of G0/G1 phase cells and augmented numbers of cells in the G2/M and S phases. Conversely, TRDMT1 knockout brought about a delayed cell cycle, which was facilitated again after further knockdown of APC (Fig. 5E, all $p < 0.05$). In a word, Sevo modulated the cell cycle by triggering the β-catenin pathway via the TRDMT1/APC pathway, thus influencing the biological behaviors of OC cells.

Inhibiting the activation of the β-catenin pathway partially reversed the regulation of Sevo on OC cell cycle, proliferation, invasion and migration

To verify that Sevo regulated OC cell biological phenotypes via stimulation of the β-catenin pathway, we knocked down β-catenin expression by cell transfection and exposed cells to Sevo for 2 h. The total β-catenin and nuclear β-catenin protein expression in OC cells were diminished (Fig. 6A-B, all $p < 0.001$), and downstream C-myc and Cyclin D1 levels were also restrained (Fig. 6C, all $p < 0.001$). Next, β-catenin knockdown partly counteracted the promotive effect produced by Sevo on the cell cycle (Fig. 6D, all $p < 0.05$). The proliferative viability, invasiveness, and migration were on downward trends, whereas the apoptotic rate was elevated in response to knockdown of β-catenin (Fig. 6E-H, all $p < 0.05$). Collectively, Sevo regulated OC cell biological malignant phenotypes by stimulating the β-catenin pathway via the TRDMT1/APC pathway.

Sevo activated the APC/β-catenin pathway to encourage OC growth in vivo via TRDMT1-mediated m5C modification

To further validate the mechanism of Sevo on OC, we subcutaneously injected OC cells pretreated with Sevo or silenced TRDMT1 into nude mice to

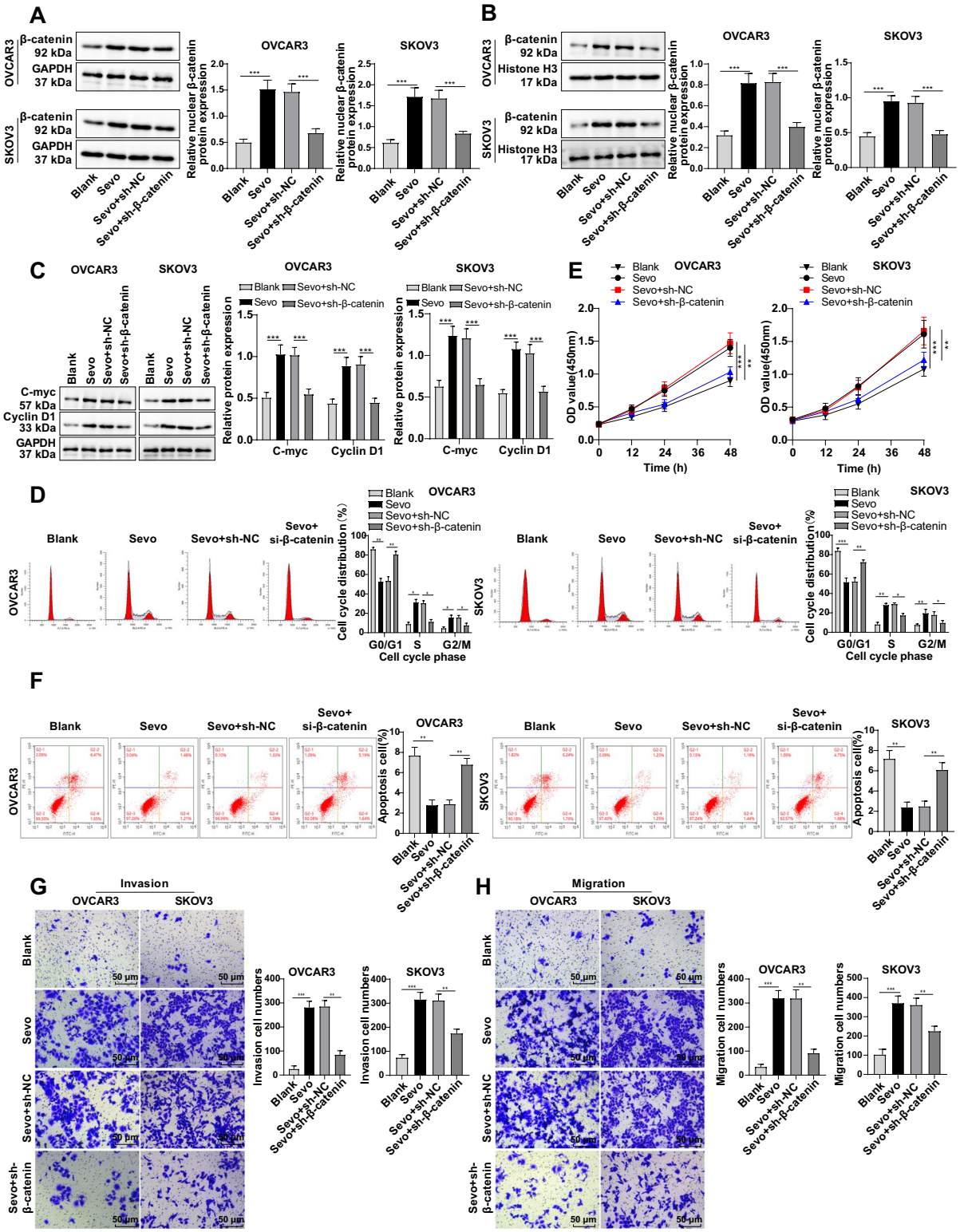
A
OVCAR3
β-catenin 92 kDa
GAPDH 37 kDa
SKOV3
β-catenin 92 kDa
GAPDH 37 kDa
Relative nuclear β-catenin protein expression
OVCAR3
SKOV3
Blank
Sevo
Sevo+sh-NC
Sevo+sh-β-catenin
B
OVCAR3
β-catenin 92 kDa
Histone H3 17 kDa
SKOV3
β-catenin 92 kDa
Histone H3 17 kDa
Relative nuclear β-catenin protein expression
OVCAR3
SKOV3
C
OVCAR3
SKOV3
C-myc 57 kDa
Cyclin D1 33 kDa
GAPDH 37 kDa
Relative protein expression
C-myc
Cyclin D1
E
OVCAR3
SKOV3
OD value(450nm)
Time (h)
D
Blank
Sevo
Sevo+sh-NC
Sevo+ si-β-catenin
OVCAR3
SKOV3
Cell cycle distribution (%)
G0/G1
S
G2/M
Cell cycle phase
F
Apoptosis cell(%)
OVCAR3
SKOV3
G
Invasion
OVCAR3
SKOV3
Invasion cell numbers
50 μm
H
Migration
OVCAR3
SKOV3
Migration cell numbers

◂**Fig. 6** Inhibiting the activation of the β-catenin pathway partially annulled the regulation of Sevo on OC cell cycle, proliferation, invasion, and migration. The interference plasmid of β-catenin was introduced into OC cells to down-regulate β-catenin expression, and the cells were subsequently subjected to Sevo treatment. **A**-**B**: Western blot assay to measure total β-catenin and intranuclear β-catenin protein levels in OC cells; **C**: Western blot assay to determine C-myc and Cyclin D1 protein levels in OC cells; **D**: Flow cytometry to detect cell cycle distribution; **E**: CCK-8 assay to evaluate cell proliferation; **F**: Flow cytometry to assess cell apoptotic rate; **G**-**H**: Transwell assay to assess cell invasion and migration. Three repeated cell experiments were performed independently, and the data were expressed as mean ± SD. One-way ANOVA was utilized for comparisons among groups. * $p < 0.05$, ** $p < 0.01$, *** $p < 0.001$

generate an animal model of OC xenograft tumor. Tumor growth within 28 days was monitored, and the results elicited that tumor volume, size, and weight were elevated in the Sevo group versus the Control group, whereas tumor growth was abated after TRDMT1 knockout (Fig. 7A-C, all $p < 0.01$). Sevo treatment augmented the percentage of ki67-positive cells, while TRDMT1 knockout subdued the positive expression of ki67 (Fig. 7D, all $p < 0.01$). Another finding was that Sevo treatment heightened TRDMT1 and β-catenin expression patterns and restricted APC expression, whereas knocking down TRDMT1 resulted in an elevated APC level and reduced β-catenin level (Fig. 7E, all $p < 0.05$). In general, Sevo could enhance OC growth in vivo by triggering the APC/β-catenin pathway through TRDMT1-mediated m5C modification.

Discussion

OC remains the most prevalent cause of mortality among gynecologic malignancies (Kujawa and Lisowska 2015; O'Shea 2022). Interestingly, evidence is accumulating regarding the role of Sevo in promoting human OC growth and exacerbating OC (Iwasaki et al. 2016; Hu et al. 2023). The present study demonstrated that the inhalational anesthetic Sevo exerted promotive effects on OC cell malignant phenotypes via the TRDMT1/m5C/APC/β-catenin axis.

It was proven that the use of 2% Sevo promotes Lewis lung cancer cell proliferation in an in vitro study (Kim et al. 2021). Furthermore, the apoptosis of oestrogen receptor-negative breast cancer cells is suppressed by post-surgery serum collected from patients who receive Sevo anesthesia (Jaura et al. 2014). Notably, the upregulation of TRDMT1 has been observed in malignancies and is linked with an unfavorable prognosis for cancer (Zhu et al. 2021). In particular, the therapeutic targeting of TRDMT1 exhibits promise in enhancing the sensitivity of OC to platinum-based therapy (Zhu et al. 2021). Nevertheless, the specific role of Sevo treatment in OC cell biological behaviors through TRDMT1 modulation remains largely unknown. Our findings for the first time disclosed that Sevo augmented TRDMT1 expression. Moreover, we uncovered that OC cells' capabilities to invade, proliferate and migrate were facilitated, whereas apoptosis and cell doubling time were reduced after Sevo exposure, but knockdown of TRDMT1 brought about opposite trends. Hence, we speculated that Sevo could up-regulate TRDMT1 expression to affect OC cell malignant phenotypes. Reportedly, Sevo promotes the colony formation, proliferation, and invasiveness of human glioblastoma cells by augmenting cell surface protein 44 (Lai et al. 2019). The absence of TRDMT1 influences the 5-methylcytosine modification of mRNA and impedes the migration and proliferation of HEK293 cells (Xue et al. 2019). Knockout of DNMT2/TRDM1 can increase doxorubicin-triggered apoptosis in breast and cervical cancer cells and become more sensitive to endoplasmic reticulum stress-induced apoptosis (Adamczyk-Grochala et al. 2023). Taken together, Sevo stimulates OC cell malignant progression via upregulation of TRDMT1.

APC is intrinsically highly-expressed in bipolar cells and brain tissues but is weakly expressed in most tumors (Zhang et al. 2022). TRDMT1 knockdown can reduce mRNA methylation, and there is evidence linking aberrant methylation of the APC gene promoter to a low level of APC protein (Sha et al. 2021; Auwera et al. 2008). Accordingly, our findings demonstrated that Sevo treatment inhibited APC expression in OC cells, and this inhibition can be mitigated by TRDMT1 knockdown. In addition, the TRDMT1 protein is accountable for facilitating the methylation of m5C in mRNA molecules, specifically at sites of DNA damage (Chen et al. 2020). Up-regulated DNMT2 gene expression has been documented to result in an elevation

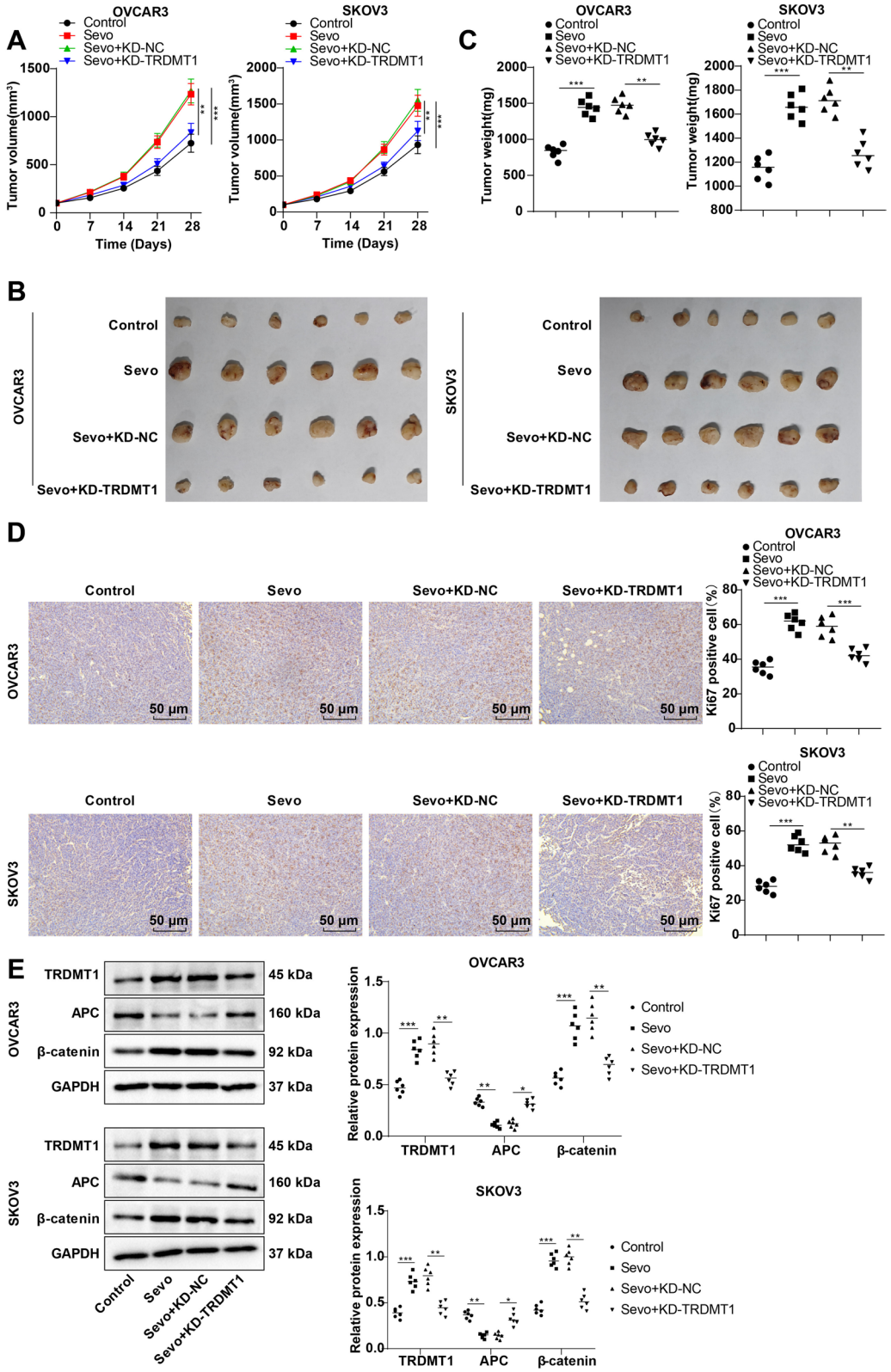
A
OVCAR3
SKOV3
Control
Sevo
Sevo+KD-NC
Sevo+KD-TRDMT1
Tumor volume(mm³)
Time (Days)
C
Tumor weight(mg)
B
D
Ki67 positive cell (%)
50 μm
E
TRDMT1
APC
β-catenin
GAPDH
45 kDa
160 kDa
92 kDa
37 kDa
Relative protein expression

◂**Fig. 7** Sevo activated the APC/β-catenin pathway to encourage OC growth in vivo through TRDMT1-mediated m5C modification. Sevo-pretreated OC cells or TRDMT1-knockdown OC cells were injected subcutaneously into nude mice to develop an animal OC xenograft tumor model. **A**: The change of tumor volume within 28 days was monitored; **B**: The size of tumor formation was observed; **C**: The final weight of the tumor was weighted; **D**: Immunohistochemistry to detect the Ki67 positive expression rate in tumor tissues; **E**: Western blot to test the protein levels of TRDMT1, APC, and β-catenin in tumor tissues. $n = 6$. Data were expressed as mean ± SD. One-way ANOVA was utilized for comparisons among groups. * $p < 0.05$, ** $p < 0.01$, *** $p < 0.001$

of RNA m5C modifications (Bohnsack et al. 2019). In agreement with the preceding research, our results elicited that the m5C methylation level of APC mRNA rose after treatment with Sevo but dropped when TRDMT1 was knocked down. Sevo is proven to generate degradation by interacting with carbon dioxide absorbents (Frink et al. 1992). Similarly, our study validated that Sevo enhanced APC mRNA degradation, while knockdown of TRDMT1 reinforced APC mRNA stability. Collectively, Sevo represses APC mRNA expression by up-regulating TRDMT1 to stimulate m5C modification of APC mRNA.

The APC protein is a tumor suppressor protein with many domains that are indispensable in regulating various cellular biological behaviors, including cell adhesion, proliferation, and migration (Zhang and Shay 2017). Furthermore, mice with reduced APC expression exhibit elevated aerobic glycolysis, squamous cell carcinoma proliferation, and tumor progression (Wang et al. 2021). Consistent with the above evidence, our findings uncovered that reduced APC expression showed involvement in elevated migration, proliferation, invasion and cell colony number, along with diminished apoptosis rate, cell doubling time and cell scratch healing ability in OC cells. Besides, Sevo could hinder APC expression by regulating TRDMT1 to boost m5C modification of APC mRNA, as we discussed before. Consequently, Sevo promotes OC cell metastasis, proliferation, and invasion and inhibits apoptosis via modulation of TRDMT1/APC expression.

Furthermore, APC is a component of the Wnt signal system, and it possesses the capacity to modulate β-catenin level (Kuraguchi et al. 2006). Downstream genes like Cyclin D1 and C-myc, are activated by the loss of APC activity and stabilized β-catenin (Yang et al. 2012; Yang et al. 2011). Cyclin D1 facilitates the progression of the cell cycle, whereas c-myc stimulates aerobic glycolysis via upregulating genes involving glycolysis (Wang et al. 2021). Mechanically, the alterations in the APC gene can stabilize and activate β-catenin, which leads to its nuclear accumulation and the constitutive activation of c-myc and cyclin D1 (Wang et al. 2018). Unsurprisingly, we noted that Sevo could activate β-catenin and up-regulate Cyclin D1, β-catenin and C-myc levels, which were bound up with its modulation of cell cycle progression, conforming to the existing evidence (Davidson and Niehrs 2010; Sherr 1996; Shtutman et al. 1999). Moreover, Sevo regulates APC expression via TRDMT1-mediated m5C modification, and APC is implicated in apoptosis, cell cycle regulation, migration, and differentiation by means of β-catenin activation in colon cancer (Zhang et al. 2016). However, down-regulated APC did not significantly affect the expression of TRDMT1, demonstrating that APC is downstream of TRDMT1. On the other hand, drug-induced G2/M cell cycle arrest is enhanced via DNMT2/TRDMT1 gene knockdown in breast cancer and glioblastoma cells (Bloniarz et al. 2021). In short, Sevo regulates cell cycle progression through the β-catenin/TRDMT1/APC pathway.

The Wnt/β-catenin pathway is a remarkably conserved signaling network that encompasses Wnt proteins, intracellular proteins like Dishevelled and APC, as well as transcription factors including β-catenin and T-cell and lymphoid enhancer factor (Maguschak and Ressler 2012; Mulligan and Cheyette 2012). As reported, colorectal cancer cell proliferation, spread, and invasiveness are effectively suppressed by limiting the Wnt/β-catenin pathway (Xu et al. 2016). After β-catenin interference plasmid was transfected into OC cells, our results displayed attenuated OC cell proliferative vitality, invasion, and migration, together with an incremental cell apoptosis rate, indicating that knockdown of β-catenin could partly counteract the regulatory effects of Sevo on OC cell biological functions. Similar effects have been observed in other studies; for instance, inhibiting β-catenin curbs cell proliferation and facilitates cell death in diverse soft tissue sarcoma cell lines (Martinez-Font et al. 2020). Shortly, β-catenin inhibition

exerts reversible effects for the regulations of Sevo on OC cell cycle, invasion, migration, and growth. Lastly, we subcutaneously injected Sevo-pretreated OC cells or TRDMT1-knockdown OC cells into nude mice to develop OC xenograft tumor animal models. The findings disclosed similar results as cell experiments that Sevo therapy up-regulated TRDMT1 and β-catenin expression levels and down-regulated APC expression, whereas after TRDMT1 expression was suppressed, APC level rose and β-catenin level fell, which suggested that Sevo could activate the APC/β-catenin pathway through TRDMT1-mediated m5C modification to promote OC growth in vivo.

Evidence suggests that Sevo can promote the proliferation and migration of ovarian cancer in a variety of ways. Masashi Ishikawa and his colleagues reported for the first time that exposure of ovarian cancer cells to volatile anesthetics such as desflurane, sevoflurane, and isoflurane could accelerate cell migration, which was eliminated by CXCR2 knockout (Iwasaki et al. 2016). Then, they found that Sevo could enhance ovarian cancer cell proliferation and migration by down-regulating miR-210 and miR-138 (Ishikawa et al. 2021). Recent data have suggested that Sevo can up-regulate GLUT1, MPC1, and GLUD1 expression levels in ovarian cancer cells, augment the Erk pathway and HIF-1α expression to modulate glucose metabolism and signal transduction, hence promoting the malignant progression of ovarian cancer (Hu et al. 2023). The above evidence indicates that Sevo can regulate ovarian cancer malignant behaviors through various mechanisms. Nonetheless, there are still few studies on the role and mechanism of Sevo in promoting ovarian cancer and other cancers. Numerous studies have reported that TRDMT1 is regulated by various stress responses (Bloniarz et al. 2021; Li et al. 2022; Thiagarajan et al. 2011). We found that Sevo stimulation induced TRDMT1 expression in our preliminary experiments, and therefore further investigated the mechanism by which Sevo regulated TRDMT1 expression to promote the malignant behaviors of ovarian cancer, which was one of the most important innovations of this study. However, the exact mechanism by which Sevo induces TRDMT1 expression is not clear, which is one of the limitations of this study. We will further delve into the molecular mechanism of Sevo-induced TRDMT1 expression in subsequent studies.

In conclusion, our study first investigates the effects of Sevo on OC biological behaviors and the molecular mechanism of Sevo regulating the APC/β-catenin pathway via modulating m5C methylation of APC mRNA through TRDMT1. Sevo promoted the malignant progression of OC cells via the RDMT1/APC axis. Sevo activated the APC/β-catenin pathway via TRDMT1-mediated m5C modification to strengthen OC growth in vivo. This study elucidated the possible mechanism of Sevo affecting the progression of OC for the first time. Therefore, the selection of anesthetics and their dosage and timing may be important links in the clinical treatment of cancer. However, this study encountered some limitations. For example, there is a lack of clinical data to confirm the role of Sevo in OC prognosis, the sample size of animal experiments is limited, and there is no complete mechanism verification experiment in vivo. Future studies should collect clinical data to further analyze the role of Sevo in OC prognosis and expand the scale of animal experiments to further verify the molecular mechanism of Sevo in promoting OC growth in vivo through TRDMT1-mediated m5C modification to activate the APC/β-catenin pathway.

Acknowledgements Not applicable.

Authors' contributions Xiaochen Huang is the guarantor of integrity of the entire study; Xiaochen Huang and Xuewei Lao contributed to the study concepts, study design, and definition of intellectual content, Xuewei Lao contributed to the literature research, Chengyan He and Jia Wang contributed to the manuscript preparation and Xiaochen Huang and Xuewei Lao contributed to the manuscript editing and review; Ying Pan and Chengyan He contributed to the experimental studies and data acquisition; Xuewei Lao contributed to the data analysis and statistical analysis. All authors read and approved the final manuscript.

Funding No funding was used in this study.

Data availability No datasets were generated or analysed during the current study.

Declarations

Ethics approval All animal experiments were approved by the ethics committee of The Third Bethune Hospital of Jilin University. Considerable efforts were conducted to minimize the animal number and their pain.

Consent for publication Not applicable.

Competing interests The authors declare no competing interests.

References

Adamczyk-Grochala J, Bloniarz D, Zielinska K, Lewinska A, Wnuk M. DNMT2/TRDMT1 gene knockout compromises doxorubicin-induced unfolded protein response and sensitizes cancer cells to ER stress-induced apoptosis. Apoptosis. 2023;28(1–2):166–85.

Angeles MA, Hernandez A, Perez-Benavente A, Cabarrou B, Spagnolo E, Rychlik A, et al. The effect of major postoperative complications on recurrence and long-term survival after cytoreductive surgery for ovarian cancer. Gynecol Oncol. 2022;166(1):8–17.

Atallah GA, Abd Aziz NH, Teik CK, Shafiee MN, Kampan NC. New predictive biomarkers for ovarian cancer. Diagnostics (Basel). 2021;11(3):465.

Bloniarz D, Adamczyk-Grochala J, Lewinska A, Wnuk M. The lack of functional DNMT2/TRDMT1 gene modulates cancer cell responses during drug-induced senescence. Aging (Albany NY). 2021;13(12):15833–74.

Bohnsack KE, Hobartner C, Bohnsack MT. Eukaryotic 5-methylcytosine (m(5)C) RNA Methyltransferases: Mechanisms, Cellular Functions, and Links to Disease. Genes (Basel). 2019;10(2):102.

Chen H, Yang H, Zhu X, Yadav T, Ouyang J, Truesdell SS, et al. m(5)C modification of mRNA serves a DNA damage code to promote homologous recombination. Nat Commun. 2020;11(1):2834.

Colosimo A, Curini V, Russo V, Mauro A, Bernabo N, Marchisio M, et al. Characterization, GFP gene Nucleofection, and allotransplantation in injured tendons of ovine amniotic fluid-derived stem cells. Cell Transplant. 2013;22(1):99–117.

Davidson G, Niehrs C. Emerging links between CDK cell cycle regulators and Wnt signaling. Trends Cell Biol. 2010;20(8):453–60.

Enlund M, Berglund A, Andreasson K, Cicek C, Enlund A, Bergkvist L. The choice of anaesthetic–sevoflurane or propofol–and outcome from cancer surgery: a retrospective analysis. Ups J Med Sci. 2014;119(3):251–61.

Fang X, Svitkina TM. Adenomatous Polyposis Coli (APC) in cell migration. Eur J Cell Biol. 2022;101(3):151228.

Frink EJ Jr, Malan TP, Morgan SE, Brown EA, Malcomson M, Brown BR Jr. Quantification of the degradation products of sevoflurane in two CO2 absorbants during low-flow anesthesia in surgical patients. Anesthesiology. 1992;77(6):1064–9.

Goll MG, Kirpekar F, Maggert KA, Yoder JA, Hsieh CL, Zhang X, et al. Methylation of tRNAAsp by the DNA methyltransferase homolog Dnmt2. Science. 2006;311(5759):395–8.

Guo G, Pan K, Fang S, Ye L, Tong X, Wang Z, et al. Advances in mRNA 5-methylcytosine modifications: Detection, effectors, biological functions, and clinical relevance. Mol Ther Nucleic Acids. 2021;26:575–93.

Heaney A, Buggy DJ. Can anaesthetic and analgesic techniques affect cancer recurrence or metastasis? Br J Anaesth. 2012;109(Suppl 1):i17–28.

Hermann A, Schmitt S, Jeltsch A. The human Dnmt2 has residual DNA-(cytosine-C5) methyltransferase activity. J Biol Chem. 2003;278(34):31717–21.

Horowitz M, Neeman E, Sharon E, Ben-Eliyahu S. Exploiting the critical perioperative period to improve long-term cancer outcomes. Nat Rev Clin Oncol. 2015;12(4):213–26.

Hu YL, Tee MK, Goetzl EJ, Auersperg N, Mills GB, Ferrara N, et al. Lysophosphatidic acid induction of vascular endothelial growth factor expression in human ovarian cancer cells. J Natl Cancer Inst. 2001;93(10):762–8.

Hu C, Wang B, Liu Z, Chen Q, Ishikawa M, Lin H, et al. Sevoflurane but not propofol enhances ovarian cancer cell biology through regulating cellular metabolic and signaling mechanisms. Cell Biol Toxicol. 2023;39(4):1395–411.

Ishikawa M, Iwasaki M, Zhao H, Saito J, Hu C, Sun Q, et al. Sevoflurane and desflurane exposure enhanced cell proliferation and migration in ovarian cancer cells via miR-210 and miR-138 downregulation. Int J Mol Sci. 2021;22(4):1826.

Iwasaki M, Zhao H, Jaffer T, Unwith S, Benzonana L, Lian Q, et al. Volatile anaesthetics enhance the metastasis related cellular signalling including CXCR2 of ovarian cancer cells. Oncotarget. 2016;7(18):26042–56.

Jaura AI, Flood G, Gallagher HC, Buggy DJ. Differential effects of serum from patients administered distinct anaesthetic techniques on apoptosis in breast cancer cells in vitro: a pilot study. Br J Anaesth. 2014;113(Suppl 1):i63–7.

Kang K, Wang Y. Sevoflurane inhibits proliferation and invasion of human ovarian cancer cells by regulating JNK and p38 MAPK signaling pathway. Drug Des Devel Ther. 2019;13:4451–60.

Kim Y, Yun S, Shin KA, Chung W, Ko Y, Kim YH, et al. Effects of sevoflurane on lewis lung carcinoma cell proliferation in vivo and in vitro. Medicina (Kaunas). 2021;57(1):45.

Kujawa KA, Lisowska KM. Ovarian cancer–from biology to clinic. Postepy Hig Med Dosw (Online). 2015;69:1275–90.

Kuraguchi M, Wang XP, Bronson RT, Rothenberg R, Ohene-Baah NY, Lund JJ, et al. Adenomatous polyposis coli (APC) is required for normal development of skin and thymus. PLoS Genet. 2006;2(9):e146.

Lai RC, Shan WR, Zhou D, Zeng XQ, Zuo K, Pan DF, et al. Sevoflurane promotes migration, invasion, and colony-forming ability of human glioblastoma cells possibly via increasing the expression of cell surface protein 44. Acta Pharmacol Sin. 2019;40(11):1424–35.

Lewinska A, Adamczyk-Grochala J, Kwasniewicz E, Deregowska A, Semik E, Zabek T, et al. Reduced levels of methyltransferase DNMT2 sensitize human fibroblasts to oxidative stress and DNA damage that is accompanied by changes in proliferation-related miRNA expression. Redox Biol. 2018;14:20–34.

Li J, Huang Y, Yang X, Zhou Y, Zhou Y. RNAm 5Cfinder: A Web-server for Predicting RNA 5-methylcytosine (m5C) Sites Based on Random Forest. Sci Rep. 2018;8(1):17299.

Li Z, Qi X, Zhang X, Yu L, Gao L, Kong W, et al. TRDMT1 exhibited protective effects against LPS-induced inflammation in rats through TLR4-NF-kappaB/MAPK-TNF-alpha pathway. Animal Model Exp Med. 2022;5(2):172–82.

Liu Z, Lu H, He G, Ma H, Wang J. Non-steroidal anti-inflammatory drugs reduce the stress response during sevoflurane anesthesia. Acta Anaesthesiol Scand. 2012;56(7):890–5.

Luo G, Xu W, Chen X, Wang S, Wang J, Dong F, et al. NSUN2-mediated RNA m(5)C modification modulates uveal melanoma cell proliferation and migration. Epigenetics. 2022;17(8):922–33.

Maguschak KA, Ressler KJ. A role for WNT/beta-catenin signaling in the neural mechanisms of behavior. J Neuroimmune Pharmacol. 2012;7(4):763–73.

Marana E, Russo A, Colicci S, Polidori L, Bevilacqua F, Viviani D, et al. Desflurane versus sevoflurane: a comparison on stress response. Minerva Anestesiol. 2013;79(1):7–14.

Martinez-Font E, Perez-Capo M, Ramos R, Felipe I, Garcias C, Luna P, et al. Impact of Wnt/beta-Catenin Inhibition on Cell Proliferation through CDC25A Downregulation in Soft Tissue Sarcomas. Cancers (Basel). 2020;12(9):2556.

Mulligan KA, Cheyette BN. Wnt signaling in vertebrate neural development and function. J Neuroimmune Pharmacol. 2012;7(4):774–87.

Muranevich SA, Polosatov MV, Rozengart EV. Enkephalins and their synthetic analogs as noncompetitive reversible inhibitors of acetylcholinesterase. Dokl Akad Nauk SSSR. 1988;298(5):1260–3.

Mytych J, Lewinska A, Bielak-Zmijewska A, Grabowska W, Zebrowski J, Wnuk M. Nanodiamond-mediated impairment of nucleolar activity is accompanied by oxidative stress and DNMT2 upregulation in human cervical carcinoma cells. Chem Biol Interact. 2014;220:51–63.

Nguyen VHL, Hough R, Bernaudo S, Peng C. Wnt/beta-catenin signalling in ovarian cancer: Insights into its hyperactivation and function in tumorigenesis. J Ovarian Res. 2019;12(1):122.

Noe O, Filipiak L, Royfman R, Campbell A, Lin L, Hamouda D, et al. Adenomatous polyposis coli in cancer and therapeutic implications. Oncol Rev. 2021;15(1):534.

O'Shea AS. Clinical staging of ovarian cancer. Methods Mol Biol. 2022;2424:3–10.

Ranes M, Zaleska M, Sakalas S, Knight R, Guettler S. Reconstitution of the destruction complex defines roles of AXIN polymers and APC in beta-catenin capture, phosphorylation, and ubiquitylation. Mol Cell. 2021;81(16):3246-61 e11.

Schmittgen TD, Livak KJ. Analyzing real-time PCR data by the comparative C(T) method. Nat Protoc. 2008;3(6):1101–8.

Sha C, Chen L, Lin L, Li T, Wei H, Yang M, et al. TRDMT1 participates in the DNA damage repair of granulosa cells in premature ovarian failure. Aging (Albany NY). 2021;13(11):15193–213.

Shang S, Hua F, Hu ZW. The regulation of beta-catenin activity and function in cancer: therapeutic opportunities. Oncotarget. 2017;8(20):33972–89.

Sherr CJ. Cancer cell cycles. Science. 1996;274(5293):1672–7.

Shtutman M, Zhurinsky J, Simcha I, Albanese C, D'Amico M, Pestell R, et al. The cyclin D1 gene is a target of the beta-catenin/LEF-1 pathway. Proc Natl Acad Sci U S A. 1999;96(10):5522–7.

Squires JE, Patel HR, Nousch M, Sibbritt T, Humphreys DT, Parker BJ, et al. Widespread occurrence of 5-methylcytosine in human coding and non-coding RNA. Nucleic Acids Res. 2012;40(11):5023–33.

Sun X, Huang X, Lu X, Wang N, Wu D, Yuan M, et al. The expression and clinical significance of the tRNA aspartic acid methyltransferase 1 protein in gastric cancer. Int J Clin Oncol. 2021;26(12):2229–36.

Takeyama E, Miyo M, Matsumoto H, Tatsumi K, Amano E, Hirao M, et al. Long-term survival differences between sevoflurane and propofol use in general anesthesia for gynecologic cancer surgery. J Anesth. 2021;35(4):495–504.

Thiagarajan D, Dev RR, Khosla S. The DNA methyltranferase Dnmt2 participates in RNA processing during cellular stress. Epigenetics. 2011;6(1):103–13.

Tuorto F, Liebers R, Musch T, Schaefer M, Hofmann S, Kellner S, et al. RNA cytosine methylation by Dnmt2 and NSun2 promotes tRNA stability and protein synthesis. Nat Struct Mol Biol. 2012;19(9):900–5.

Van der Auwera I, Van Laere SJ, Van den Bosch SM, Van den Eynden GG, Trinh BX, van Dam PA, et al. Aberrant methylation of the Adenomatous Polyposis Coli (APC) gene promoter is associated with the inflammatory breast cancer phenotype. Br J Cancer. 2008;99(10):1735–42.

Wang X, Xu C, Hua Y, Cheng K, Zhang Y, Liu J, et al. Psoralen induced cell cycle arrest by modulating Wnt/beta-catenin pathway in breast cancer cells. Sci Rep. 2018;8(1):14001.

Wang W, Shao F, Yang X, Wang J, Zhu R, Yang Y, et al. METTL3 promotes tumour development by decreasing APC expression mediated by APC mRNA N(6)-methyladenosine-dependent YTHDF binding. Nat Commun. 2021;12(1):3803.

Xu Z, Qian B. Sevoflurane anesthesia-mediated oxidative stress and cognitive impairment in hippocampal neurons of old rats can be ameliorated by expression of brain derived neurotrophic factor. Neurosci Lett. 2020;721:134785.

Xu M, Wang S, Song YU, Yao J, Huang K, Zhu X. Apigenin suppresses colorectal cancer cell proliferation, migration and invasion via inhibition of the Wnt/beta-catenin signaling pathway. Oncol Lett. 2016;11(5):3075–80.

Xue S, Xu H, Sun Z, Shen H, Chen S, Ouyang J, et al. Depletion of TRDMT1 affects 5-methylcytosine modification of mRNA and inhibits HEK293 cell proliferation and migration. Biochem Biophys Res Commun. 2019;520(1):60–6.

Yang W, Xia Y, Ji H, Zheng Y, Liang J, Huang W, et al. Nuclear PKM2 regulates beta-catenin transactivation upon EGFR activation. Nature. 2011;480(7375):118–22.

Yang W, Xia Y, Hawke D, Li X, Liang J, Xing D, et al. PKM2 phosphorylates histone H3 and promotes gene transcription and tumorigenesis. Cell. 2012;150(4):685–96.

Zhang L, Shay JW. Multiple roles of APC and its therapeutic implications in colorectal cancer. J Natl Cancer Inst. 2017;109(8):djw332.

Zhang L, Theodoropoulos PC, Eskiocak U, Wang W, Moon YA, Posner B, et al. Selective targeting of mutant adenomatous polyposis coli (APC) in colorectal cancer. Sci Transl Med. 2016;8(361):361ra140.

Zhang C, Wang B, Wang X, Sheng X, Cui Y. Sevoflurane inhibits the progression of ovarian cancer through down-regulating stanniocalcin 1 (STC1). Cancer Cell Int. 2019;19:339.

Zhang Y, Liu X, Li A, Tang X. A pan-cancer analysis on the carcinogenic effect of human adenomatous polyposis coli. PLoS ONE. 2022;17(3):e0265655.

Zhu X, Wang X, Yan W, Yang H, Xiang Y, Lv F, et al. Ubiquitination-mediated degradation of TRDMT1 regulates homologous recombination and therapeutic response. NAR Cancer. 2021;3(1):zcab010.